AGU PUBLICATIONS

Geophysical Research Letters

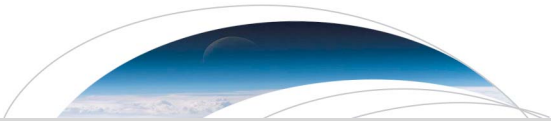

RESEARCH LETTER

10.1002/2017GL076166

Key Points:

- First successful detection of spaceborne GNSS-Reflectometry signals in hurricanes
- Evidence of GNSS-R sensitivity to hurricane structure
- Retrieval of credible GNSS-R wind speed near hurricane inner core

Correspondence to:
G. Foti,
g.foti@noc.ac.uk

Citation:
Foti, G., Gommenginger, C., & Srokosz, M. (2017). First spaceborne GNSS-Reflectometry observations of hurricanes from the UK TechDemoSat-1 mission. *Geophysical Research Letters*, *44*, 12,358–12,366. https://doi.org/10.1002/2017GL076166

Received 24 OCT 2017
Accepted 4 DEC 2017
Accepted article online 8 DEC 2017
Published online 26 DEC 2017

First Spaceborne GNSS-Reflectometry Observations of Hurricanes From the UK TechDemoSat-1 Mission

Giuseppe Foti[1], **Christine Gommenginger**[1], **and Meric Srokosz**[1]

[1]National Oceanography Centre, Southampton, UK

Abstract We present the first examples of Global Navigation Satellite Systems-Reflectometry (GNSS-R) observations of hurricanes using spaceborne data from the UK TechDemoSat-1 (TDS-1) mission. We confirm that GNSS-R signals can detect ocean condition changes in very high near-surface ocean wind associated with hurricanes. TDS-1 GNSS-R reflections were collocated with International Best Track Archive for Climate Stewardship (IBTrACS) hurricane data, MetOp ASCAT A/B scatterometer winds, and two reanalysis products. Clear variations of GNSS-R reflected power (σ^0) are observed as reflections travel through hurricanes, in some cases up to and through the eye wall. The GNSS-R reflected power is tentatively inverted to estimate wind speed using the TDS-1 baseline wind retrieval algorithm developed for low to moderate winds. Despite this, TDS-1 GNSS-R winds through the hurricanes show closer agreement with IBTrACS estimates than winds provided by scatterometers and reanalyses. GNSS-R wind profiles show realistic spatial patterns and sharp gradients that are consistent with expected structures around the eye of tropical cyclones.

1. Introduction

Hurricanes, typhoons, and cyclones (all denominations of the same weather phenomenon) are recognized as one of the potentially most destructive forces in nature, so observing and predicting their behavior has been an on-going ambition and challenge (Gall et al., 2013; Mohanty & Gopalakrishnan, 2016). The recent devastating impact of hurricanes Harvey on Houston and Irma on Florida and the Caribbean underlines the need for improved observations and predictions. Theoretical advances continue to be made (Montgomery & Smith, 2017), but progress also depends on obtaining good observations, particularly near the inner core. Here we demonstrate for the first time that useful observations of hurricanes can be obtained using spaceborne Global Navigation Satellite System-Reflectometry (GNSS-R). GNSS-R is a relatively new remote sensing technique (Zavorotny et al., 2014), whose utility for measuring hurricane winds has previously been demonstrated only using airborne GNSS-R systems (Katzberg et al., 2006). In this paper, we present examples from the UK TechDemoSat-1 (TDS-1) mission that demonstrates for the first time that GNSS-R can sense ocean surface condition changes associated with hurricanes using spaceborne receivers. We also show that, once GNSS-R signals are corrected for instrument and platform effects, credible wind speed profiles that are consistent with expected hurricane wind field structures and gradients can be retrieved in hurricanes from spaceborne GNSS-R signals.

The measurement of wind speeds in hurricanes has a long history, and a variety of techniques have been used (e.g., Kishtawal, 2016; Marks, 2016). Even today, the key measurement challenges are still to obtain accurate wind speed data with sufficient temporal and spatial resolution, and in the presence of heavy precipitation. The sampling challenge is particularly critical given the potential of hurricanes for both fast development and fast translation. Given the large number of transmitters in Global Navigational Satellite Systems such as GPS, GLONASS, or Galileo, spaceborne GNSS-R has the potential to alleviate the sampling problems if sufficient number of GNSS-R receivers can be flown in space. In addition, by operating in the L-band microwave frequency range, GNSS-R is much less affected by heavy precipitation than other spaceborne measurement techniques such as scatterometry, which operates at higher microwave frequencies (e.g., Quilfen et al., 1998). These observational requirements for fast-revisit and high performance in heavy precipitation were the main motivation for the constellation of eight small satellites launched for the NASA Cyclone Global Navigation Satellite System (CYGNSS) in December 2016 (Ruf et al., 2016).

The potential for GNSS-R measurements to deliver wind speed data in hurricanes has been demonstrated previously in a series of airborne experiments stretching back almost 20 years (Lin et al., 1999; Katzberg et al., 2001, 2006; Katzberg & Dunion, 2009). These studies have shown that wind speeds measurements could be

made up to ~40 m/s (Katzberg et al., 2006; Katzberg & Dunion, 2009). However, given that GNSS-R signals become weaker with increasing winds and increasing altitude, it was not evident until now that GNSS-R would retain enough sensitivity to sense surface condition changes in very high near-surface wind conditions associated with hurricanes when operating from spaceborne platforms.

In this paper, we present the first examples of hurricanes successfully observed with GNSS-R measurements from space using data from the TechDemoSat-1 (TDS-1) mission. Since we limit ourselves to TDS-1, we cannot consider issues of space-time sampling of hurricanes. Instead, we focus on exploring whether spaceborne GNSS-R can (a) sense surface condition changes within hurricanes; and (b) provide credible wind speed measurements in hurricanes. These questions are addressed by examining GNSS-R signals for a small number of hurricane case studies sampled by TDS-1. Ancillary information from hurricane forecasting centers, scatterometers and re-analyses about the location and structure of hurricanes serves to confirm that GNSS-R reflected power is clearly able to detect changes in surface conditions linked to hurricanes. Next, the GNSS-R reflected power is inverted to retrieve estimates of wind speed using the baseline inversion algorithm developed for TDS-1 in low to moderate winds. Even though the validity of the inversion at high winds is not known, we find that the retrieved GNSS-R winds offer credible wind field magnitude and structures.

The remainder of the paper is structured as follows. In section 2, a description of the data and methods used in this paper is given. The results from our case studies are described in section 3. Finally, in sections 4 and 5 of the paper, we discuss the results and give the conclusions of the study.

2. Data and Methods

This paper investigates the sensitivity to ocean surface parameters and wind retrieval capability of spaceborne GNSS-R signals in the presence of very high near-surface ocean winds associated with hurricanes. For this purpose, GNSS-R reflections collected by the TDS-1 mission were collocated with tropical storm data of the International Best Track Archive for Climate Stewardship (IBTrACS), with measurements from the MetOp ASCAT A/B scatterometers, and with climate reanalyses of the European Centre for Medium-Range Weather Forecasts (ECMWF ERA-Interim) and the Japanese Meteorological Agency (JMA JRA-55). IBTrACS data were obtained from the National Centers for Environment Information of the National Oceanic and Atmospheric Administration (NOAA) via their online portal (http://www.ncdc.noaa.gov/ibtracs); ASCAT A/B orbital granules were retrieved from the NASA Physical Oceanography Distributed Active Archive Center (PODAAC; http://podaac.jpl.nasa.gov); ECMWF surface winds reanalysis data were downloaded from the Centre's online dissemination platform (http://apps.ecmwf.int/datasets/); and JMA model winds were sourced from the Research Data Archive of the University Corporation for Atmospheric Research (UCAR) found at https://rda.ucar.edu.

2.1. TDS-1

The TechDemoSat-1 satellite was successfully launched on 8 July 2014. TDS-1 is a UK-funded technology demonstrator satellite, which carries eight experimental payloads including the Space GNSS Receiver Remote Sensing Instrument (SGR-ReSI). The TDS-1 satellite was placed into orbit at an altitude around 635 km with an inclination of 98.4°. The orbit is quasi Sun-synchronous. The satellite is controlled and operated from the ground station with a strict 8 day duty cycle shared between the eight experimental payloads. The SGR-ReSI can be accessed and operated for only 2 days in every 8 day cycle. The baseline operation of the ReSI is for continuous acquisition of delay-Doppler maps (DDMs) generated onboard at 1 Hz with a coherent integration time of 1 ms. For more details of the satellite and instrument, see Unwin et al. (2016) and Foti et al. (2015), and references therein.

The GNSS-R instrument flying on the TDS-1 platform is built around the SGR-ReSI receiver (Foti et al., 2015; Unwin et al., 2016), which can be operated in two modes: Automatic Gain Mode (AGM) or Programmed Gain Mode (PGM) (Foti et al., 2017). Here only GNSS-R data collected with the receiver operating in Programmed Gain Mode (PGM) are included in the analysis, as this allows for the application of absolute radiometric calibration. The PGM GNSS-R data used for analysis correspond to TDS-1 catalogs RD28 to RD87 collected from May 2015 until the beginning of October 2016, and amounting to a total of over 26 million 1 Hz Delay-Doppler Maps (DDM).

GNSS-R estimates of near-surface wind speed are obtained using a semiempirical retrieval algorithm developed at the National Oceanography Centre for radiometrically calibrated GNSS-R observables. Based on the earlier work of Foti et al. (2015), the inversion uses the bistatic radar equation to account for viewing geometry and applies corrections linked to the TDS-1 receiver antenna pattern and variability of the direct signal power level from GNSS transmitters. One point to note is that the wind speed algorithm has been developed using a matchup data set with ASCAT (Foti et al., 2015), but since ASCAT measurements are not deemed reliable beyond 25–30 m/s (Fernandez et al., 2006; Figa-Saldaña et al., 2002), the validity of the baseline TDS-1 Geophysical Model Function (GMF) developed for low-to-moderate winds is not known beyond that range of wind speeds. This uncertainty about the GMF at high winds is a common problem for all remote sensing techniques attempting to measure extreme winds and is related to the general shortage of reliable validation data in high wind conditions to develop and validate the GMF at high winds. Thus, we proceed with caution with this baseline GMF, bearing in mind that the magnitude of the wind speed will be subject to the uncertainties about the GMF at high winds. For the same reason, when presenting the results below, we start by considering the response of the GNSS-R reflected power, as represented by the bistatic radar cross section, σ^0, as the tracks travel across the hurricanes, before looking at the retrieved wind speeds.

2.2. Ancillary Data

IBTrACS data included in this analysis correspond to global records of tropical cyclones (TC) that occurred in the years 2015 and 2016. Tropical cyclone estimates available from IBTrACS include location of the center of the storm, maximum wind speed, and TC radius relative to a reference wind speed. A total of ~3,000 tropical cyclone records along the track of 64 separate storms were examined. Of these, only tropical cyclone records with estimated maximum winds above 30 m/s were retained for further analysis and collocation with the TDS-1 satellite. Overpasses of TDS-1 above tropical cyclones were defined such that the specular point of the GNSS-R instrument footprint and the IBTrACS storm center were collocated within a radius of 300 km (~3°) and a maximum temporal offset of 6 h. Applying these criteria, a total of 33 crossovers between TDS-1 and hurricanes were identified over the study period (May 2015–October 2016).

It should be noted that using IBTrACS data as ground truth for satellite measurements is subject to a number of limitations in its own right, including: (a) Best Track intensity estimates are largely based on the Dvorak technique that uses cloud patterns to infer the maximum wind speed (associated uncertainties of the order of 10%) (Knaff et al., 2010); (b) Best Track wind speed generally refers to 1 min sustained maximum winds (Knaff et al., 2010), whereas roughness-based satellite measurements typically represent longer time scales associated with the dynamics of sea surface roughness/wave development. For this reason, the analyses also use data from satellite scatterometers and reanalysis products.

Scatterometer measurements from the ASCAT instruments on the MetOp-A and MetOp-B tandem missions consisted of globally distributed 25 km L2 wind speed swath data from May 2015 to October 2016. The criteria for collocation between ASCAT A/B and TDS-1 were for maximum separation of 1° and 1 h. In case of multiple collocations in space within 1 h, the ASCAT observation with the shorter temporal offset was selected.

Surface wind speed from state-of-the-art climate reanalyses from ECMWF (ERA-Interim) and JMA (JRA-55) were obtained as detailed above. Reanalysis data were collocated with TDS-1 by selecting model data that are spatiotemporally closest to the specular point and time of acquisition of TDS-1. The collocation criteria between TDS-1 and the reanalyses correspond to the spatiotemporal resolution of the model, specifically 0.75° and 6 h for ERA-Interim, and 0.5° and 6 h for JRA-55. Some of the skills and limitations of global climate reanalysis products when applied to the study of tropical cyclones have been described in previous studies (e.g., Murakami, 2014).

3. Results

Following the application of the data selection and collocation criteria detailed above, only five examples of TDS-1 GNSS-R tracks intercepting hurricanes remained that were suitable for further analysis, the main limitation being the availability of a sufficient amount of collocated ASCAT measurements over the hurricane for comparison. The examples that are retained are from four tropical cyclones that occurred in 2015 and were named: Joaquin, Jimena, Dolphin (two crossovers), and Chan-Hom. Here, for the sake of brevity, we present

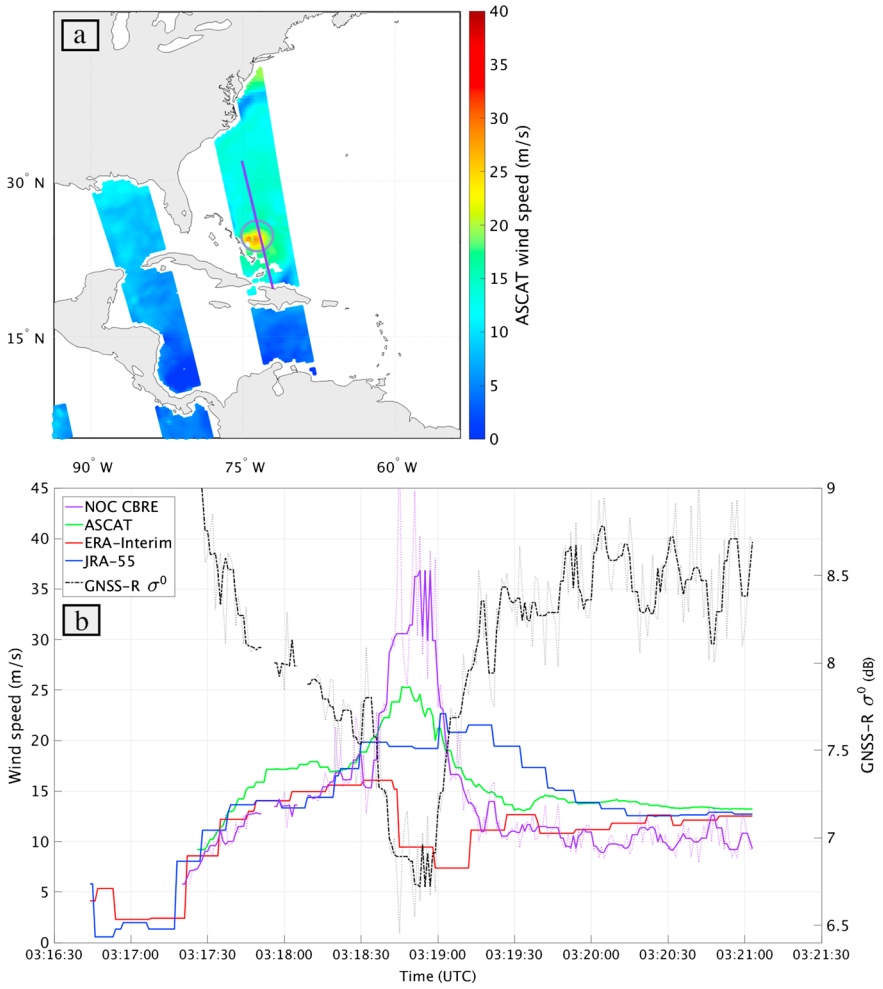

Figure 1. TDS-1 overpass (RD48, track 1111) over tropical cyclone Joaquin in the Western Atlantic (24.8 N 73.6 W) on 3 October 2015. (a) A georeferenced map with the IBTrACS location of the center of the cyclone and search radius (circle), TDS-1 track (purple) and collocated ASCAT-B wind speed swath. (b) Along-track TDS-1 σ^0 (black; right-hand scale) at 1 Hz (dashed line) and 0.2 Hz (solid line), along-track TDS-1 wind speed estimated using the NOC calibrated bistatic radar equation (NOC CBRE) algorithm (purple; left-hand scale), ASCAT (green), ECMWF ERA-interim (red), and JRA-55 (blue).

results only from Joaquin, Jimena, and Chan-Hom to show the abilities of GNSS-R to obtain data and retrieve wind speeds in hurricanes. The examples from Dolphin are not presented here as the wind speeds were lower and the collocations between TDS-1 and ASCAT were not as good, but the results were similar to those for Joaquin, Jimena, and Chan-Hom that are discussed next.

The three hurricanes are studied sequentially: first, Joaquin; second, Jimena; and third, Chan-Hom. Joaquin was observed with TDS-1 on 3 October 2015 in the subtropical North West Atlantic; TDS-1 observation of Jimena were made on 1 September 2015 in the tropical North Pacific. Finally, Chan-Hom observations with TDS-1 were made on 7 July 2015 in the tropical North Pacific. The possible occurrence of rapid storm intensification or deintensification was considered through analysis of the maximum wind speed reported by the IBTrACS estimates immediately adjacent (−6 h, +6 h) to the collocated GNSS-R observations. In all three cases presented, no indication of rapid storm intensity change was found within this collocation window.

3.1. Joaquin

Figure 1 shows the crossover between TDS-1 (RD48, Track 1111) and tropical cyclone Joaquin in the subtropical North West Atlantic (24.8 N 73.6 W) on 3 October 2015. Figure 1a shows a georeferenced map with the IBTrACS location of the center of the cyclone, the TDS-1 track and the collocated ASCAT-B wind speed swath. To show that spaceborne GNSS-R is capable of retrieving useful signals in hurricane conditions, Figure 1b

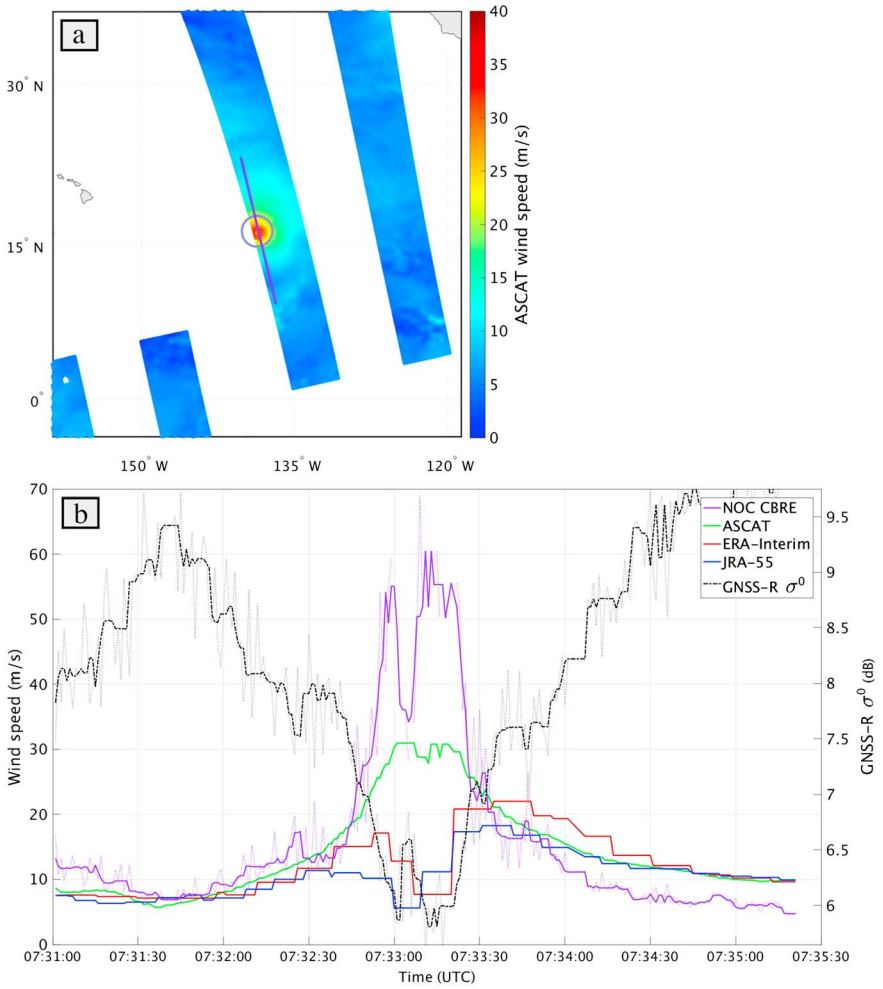

Figure 2. TDS-1 overpass (RD44, track 1250) over tropical cyclone Jimena in the eastern Pacific (16.3 N 138.7 W) on 1 September 2015. Legend as in Figure 1.

shows the along-track evolution of σ^0 through the hurricane. The σ^0 is shown both at 1 Hz (the original data posting for TDS-1; dashed lines) and as a 5 s along-track running mean (to match the 25–30 km footprint size of the GNSS-R measurement; solid lines). Of note are the high values of σ^0 away from the eye and the decrease as the center of cyclone is approached. This is as expected, given that σ^0 is inversely related to the wind speed (Foti et al., 2015), and increasing wind speed toward the center of a hurricane. Note that, in the case of Joaquin, the TDS-1 observations do not pass directly through the eye of the hurricane.

Figure 1b also presents the along-track collocated wind speed estimates reported by TDS-1, again both at 1 Hz and as a 5 s running mean, together with winds from ASCAT, ECMWF ERA-Interim, and JMA JRA-55. IBTrACS reports a maximum wind speed equal to 61.7 m/s, whereas the maximum speed indicated by ASCAT is ~26 m/s along the TDS-1 track, and only slightly higher (28.7 m/s) over the full swath enclosing the center of the storm. TDS-1 wind speeds reach ~45 m/s, significantly higher than the reanalyses or scatterometer wind speeds. The missing data seen in the initial part of the TDS-1 profile are associated with two small Caribbean islands intercepted by the TDS-1 track.

3.2. Jimena

Next, Figure 2 presents data for the TDS-1 overpass (RD44, Track 1250) over tropical cyclone Jimena in the Eastern Pacific (16.3 N 138.7 W) on 1 September 2015. Again, the behavior of σ^0 is consistent with the expected wind variation through the hurricane, with good signal acquisition throughout the tropical cyclone (Figure 2b). Here IBTrACS estimates a maximum wind speed of 59.2 m/s, not dissimilar to that of Joaquin,

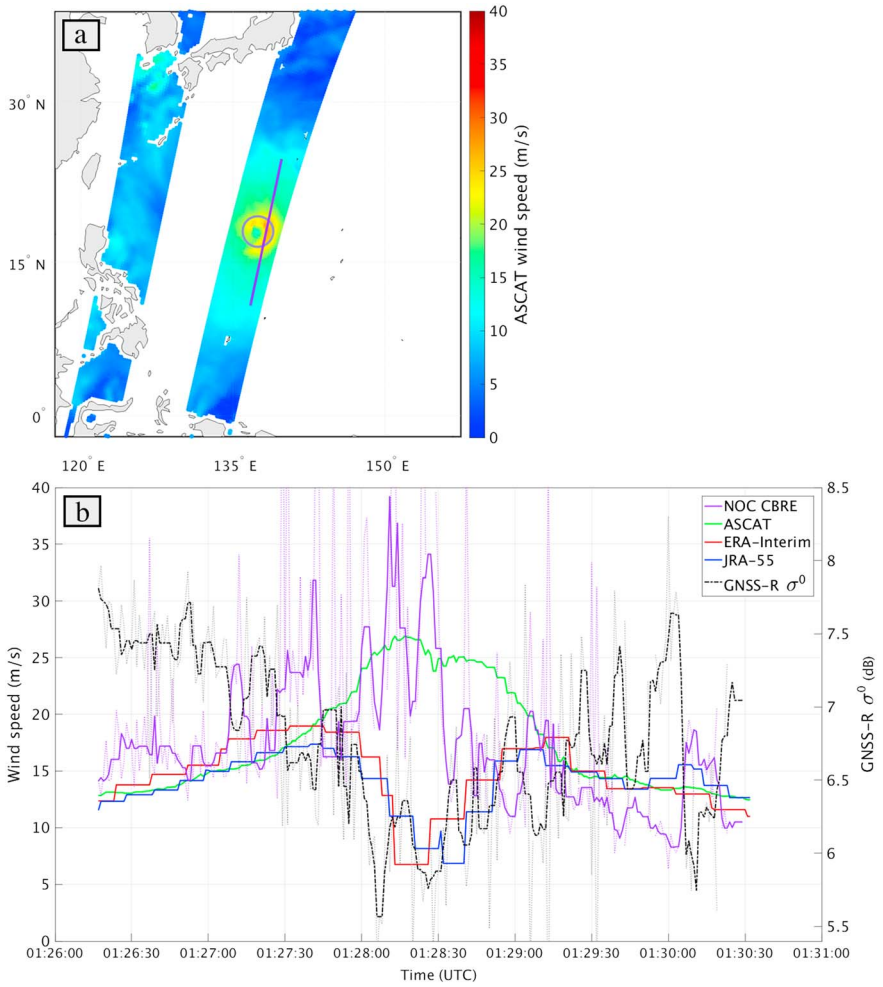

Figure 3. TDS-1 overpass (RD37, track 247) over tropical cyclone Chan-Hom in the eastern Pacific (17.9 N 137.45°E) on 7 July 2015. Legend as in Figure 1.

while collocated ASCAT winds reach only slightly above 30 m/s (maximum wind speed across the full ASCAT swath is 32.5 m/s). TDS-1 reports GNSS-R winds of almost 70 m/s near the eye wall, again exceeding both the reanalyses and scatterometer estimates and, in this case, also the maximum reported by IBTrACS. At this point, bearing in mind the uncertainty in the TDS-1 baseline GMF at high winds, we note that some 1 Hz data near the eye wall are removed by the quality control flag of the baseline algorithm which caps TDS-1 retrieved winds at 70 m/s. The key point here is that the GNSS-R σ^0 data are robust and spatially coherent right up to the eye wall, so that more trustworthy wind speeds could be derived if a validated GMF based on high wind speed validation data from a source other than ASCAT were available. Finally, it is worth noting that, in the case of Jimena, the TDS-1 observations pass through the eye of the hurricane and report wind speeds that are consistent with the lower wind speeds expected within the eye.

3.3. Chan-Hom

Finally, Figure 3 presents an analysis of TDS-1 data (RD44, Track 1250) over tropical cyclone Chan-Hom located in the Eastern Pacific (17.9 N 137.45°E) on 7 July 2015. Yet again, the behavior of σ^0 is as expected, with good signal acquisition throughout the tropical cyclone (Figure 3b). Here IBTrACS estimates a maximum wind speed of 33.4 m/s, while collocated ASCAT winds reach magnitude only slightly above 26 m/s. TDS-1 reports GNSS-R derived winds up to ~40 m/s, again exceeding the reanalyses, scatterometer and IBTrACS estimates. The same word of caution about the validity of the TDS-1 high wind speed estimates applies here.

4. Discussion

Three examples of hurricanes intercepted by TDS-1 GNSS-R tracks have been examined. In all three cases, it was seen that TDS-1 acquired good quality reflected signals across the hurricanes from which wind speed can be retrieved. This represents for the first time empirical evidence that spaceborne GNSS-R can collect useful data in hurricane conditions, which can be processed to provide additional measurements of high wind speeds.

As part of our investigations, we observed that climate reanalysis data are generally in good agreement with the wind field reported by ASCAT, at least up to a moderate-to-high speed (~15–20 m/s). At higher speeds, model winds are routinely biased low relative to ASCAT. Perhaps more importantly, reanalysis wind profiles through hurricanes do not typically capture known spatial features of tropical cyclones. This is most likely associated with the spatial resolution of the model, which cannot support the representation of finer scale structures of storms, especially in proximity of the eye.

In comparison, from the TDS-1 observations, we find that GNSS-R winds are in good agreement with ASCAT estimates up to about 20–25 m/s. Beyond that range, significant discrepancies appear: scatterometers feature maximum wind speeds around 30 m/s, in contrast to GNSS-R estimates of up to ~70 m/s. Assuming IBTrACS gives the most reliable estimates of maximum wind speeds (~60 m/s), these results suggest that scatterometers significantly underestimate the actual hurricane wind speeds, whereas GNSS-R may overestimate slightly. Given that the baseline GNSS-R wind speed algorithm has not been calibrated against high winds, it would not be surprising to find that the baseline algorithm leads to overestimation at high winds. At this point, it is not possible to conclude more fully on how well GNSS-R winds represent the magnitude of winds in hurricanes. This would require dedicated campaigns of TDS-1 observations in hurricanes for which reliable wind observations are available (e.g., from NOAA's airborne Stepped-Frequency Microwave Radiometer, SFMR), which is not the case for any of the hurricanes considered here.

So setting to one side for now the challenges linked to GNSS-R wind inversion, let us consider the results showing that GNSS-R reflected power signals are sensitive to changes in ocean surface conditions associated with the hurricane wind fields. We find that GNSS-R profiles depict features that are consistent with the structure of tropical cyclones and provide observations right up to and through the center of the storm without data loss. This confirms that useful reflections can be acquired by the TDS-1 GNSS-R receiver from low Earth orbit (635 km altitude) even in extreme wind conditions when GNSS-R signals are very weak. In addition, the availability of observations right up to the hurricane eye wall suggests that GNSS-R may indeed be less impacted by heavy precipitation, courtesy of it operating at the lower L-band microwave frequency than higher-frequency scatterometers. While we have no independent means of confirming that the TDS-1 tracks sampled heavy precipitation conditions, it is likely that at least some of the data were acquired in heavy precipitation since those are commonplace in hurricanes.

Upon closer inspection of tropical cyclone Jimena (Figure 2), we observe that the GNSS-R wind profile is able to capture sharp wind speed gradients around the tropical cyclone eye. GNSS-R wind speed increases rapidly as the track approaches the eye wall, and then decreases rapidly as the track recedes on the opposite side, successfully depicting the well-known radial symmetry of tropical cyclones. Once again, we note that the TDS-1 baseline GNSS-R wind inversion was designed to produce wind estimates with a nominal footprint size of 25 km and was never intended as a means of obtaining high-resolution observations in extreme conditions. The fact that the TDS-1 GNSS-R data depict fine-scale structures near the eye wall of the tropical cyclone opens very promising new opportunities as well as new challenges in determining the contribution that GNSS-R can make to improve our understanding of hurricanes.

5. Conclusions

In this paper we have demonstrated that spaceborne GNSS-R can provide useful ocean surface observations in hurricane conditions. GNSS-R data from the TDS-1 mission were compared with estimates of wind speed from IBTrACS, scatterometers, and reanalysis products. The key conclusions of this study are as follows:

1. For the first time, GNSS-R observations have successfully been acquired in hurricane wind conditions with a spaceborne receiver orbiting at LEO altitude.

2. GNSS-R σ^0 data show sensitivity to changes in ocean surface conditions that are consistent with wind fields expected in hurricanes.
3. GNSS-R provides observations right up to and through the eye wall without loss of data.
4. The application of the baseline TDS-1 GNSS-R wind speed inversion produces credible estimates of wind speed, even in very high to extreme wind conditions.
5. GNSS-R wind profiles through the hurricanes contain features that are consistent with known spatial structures of hurricanes.
6. Reanalysis models and scatterometer winds are consistent with each other up to moderate-to-high wind speed (~20 m/s), but both underestimated the magnitude of hurricane winds compared to IBTrACS and GNSS-R. The observed underestimation of hurricane winds by the scatterometers is consistent with previous findings (e.g., Fernandez et al., 2006, and references therein).
7. Maximum wind speeds reported by scatterometers do not exceed 35 m/s, whereas GNSS-R data can reach up to ~70 m/s, giving closer agreement with IBTrACS estimates than either models or scatterometers.

The results of this study are significant since the first three bullet points above were not a priori obvious for a spaceborne GNSS-R system such as TDS-1. The findings are directly relevant to the NASA CYGNSS mission and its scientific objectives of providing improved wind data in hurricane conditions from space.

As its name implies, TechDemoSat-1 was launched to demonstrate new technology and, in the case of GNSS-R for ocean wind sensing, it has clearly been very successful (Foti et al., 2015). This paper has shown that TDS-1 can also provide estimates of wind speed in hurricane conditions, even though the system was not specifically designed nor optimized for that purpose. Given the limited duty cycle of TDS-1 GNSS-R observations (operations for 2 days in every 8) it can only provide a limited amount of data. The CYGNSS mission, specifically designed for monitoring tropical cyclones, will provide many more measurements and should lead to significant improvements in the retrieval of wind speed in hurricanes.

In concluding we note that it is not only active L-band remote sensing, as provided by GNSS-R, which can provide measurements in hurricane conditions. Recent work (Meissner et al., 2017; Reul et al., 2012, 2016) has shown the potential of L-band passive microwave radiometry for measuring wind speed, with instruments like the Soil Moisture and Ocean Salinity (SMOS) and the Soil Moisture Active Passive (SMAP) missions, which were not designed for that purpose either. Results using SMOS and SMAP suggest that winds of up to 65 m/s can be measured. Therefore, comparing and combining GNSS-R with L-band radiometry offers the potential for further advances in wind monitoring of hurricanes.

Acknowledgments
This work was partly funded by the European Space Agency under contract RFP ESA-IPL-PEO-FF-ah-LE-2015-377 "ESA TDS-1 GNSS-R Exploitation Phase 2" and partly under NERC National Capability funding at the National Oceanography Centre. All TDS-1 L1b data used in these analyses are available freely upon registration through the MERRByS data dissemination portal at http://merrbys.co.uk, hosted and managed by Surrey Satellite Technology Ltd, Guildford, UK. All other data used in this study are publicly available from the sources quoted in the paper. We are grateful for the helpful comments from two anonymous reviewers.

References

Fernandez, D. E., Carswell, J. R., Frasier, S., Chang, P. S., Black, P. G., & Marks, F. D. (2006). Dual-polarized C- and Ku-band ocean backscatter response to hurricane-force winds. *Journal of Geophysical Research*, *111*, C08013. https://doi.org/10.1029/2005JC003048

Figa-Saldaña, J., Wilson, J. J., Attema, E., Gelsthorpe, R., Drinkwater, M. R., & Stoffelen, A. (2002). The advanced scatterometer (ASCAT) on the meteorological operational (MetOp) platform: A follow on for European wind scatterometers. *Canadian Journal of Remote Sensing*, *28*(3), 404–412. https://doi.org/10.5589/m02-035

Foti, G., Gommenginger, C., Jales, P., Unwin, M., Shaw, A., Robertson, C., & Rosello, J. (2015). Spaceborne GNSS reflectometry for ocean winds: First results from the UK TechDemoSat-1 mission. *Geophysical Research Letters*, *42*(13), 5435–5441. https://doi.org/10.1002/2015GL064204

Foti, G., Gommenginger, C., Unwin, M., Jales, P., Tye, J., & Roselló, J. (2017). An assessment of non-geophysical effects in spaceborne GNSS reflectometry data from the UK TechDemoSat-1 mission. *IEEE Journal of Selected Topics in Applied Earth Observations and Remote Sensing*, *10*(7), 3418–3429. https://doi.org/10.1109/JSTARS.2017.2674305

Gall, R., Franklin, J., Marks, F., Rappaport, E. N., & Toepfer, F. (2013). The hurricane forecast improvement project. *Bulletin of the American Meteorological Society*, *94*(3), 329–343. https://doi.org/10.1175/BAMS-D-12-00071.1

Katzberg, S. J., & Dunion, J. (2009). Comparison of reflected GPS wind speed retrievals with dropsondes in tropical cyclones. *Geophysical Research Letters*, *36*, L17602. https://doi.org/10.1029/2009GL039512

Katzberg, S. J., Torres, O., & Ganoe, G. (2006). Calibration of reflected GPS for tropical storm wind speed retrievals. *Geophysical Research Letters*, *33*, L18602. https://doi.org/10.1029/2006GL026825

Katzberg, S. J., Walker, R. A., Roles, J. H., Lynch, T., & Black, P. G. (2001). First GPS signals reflected from the interior of a tropical storm: Preliminary results from Hurricane Michael. *Geophysical Research Letters*, *28*(10), 1981–1984. https://doi.org/10.1029/2000GL012823

Kishtawal, C. M. (2016). Use of satellite observations in tropical cyclone studies. In U. C. Mohanty, & S. G. Gopalakrishnan (Eds.), *Advanced numerical modeling and data assimilation techniques for tropical cyclone prediction* (chap 2). Dordrecht, Netherlands: Springer. https://doi.org/10.5822/978-94-024-0896-6_2

Knaff, J. A., Brown, D. P., Courtney, J., Gallina, G. M., & Beven, J. L. II (2010). An evaluation of Dvorak technique-based tropical cyclone intensity estimates. *Weather and Forecasting*, *25*(5), 1362–1379. https://doi.org/10.1175/2010WAF2222375.1

Lin, B., Katzberg, S. J., Garrison, J. L., & Wielicki, B. A. (1999). Relationship between GPS signals reflected from sea surfaces and surface winds: Modeling results and comparisons with aircraft measurements. *Journal of Geophysical Research*, *104*(C9), 20713–20727. https://doi.org/10.1029/1999JC900176

Marks, F. D. (2016). Advancing the understanding and prediction of tropical cyclones using aircraft observations. In U. C. Mohanty, & S. G. Gopalakrishnan (Eds.), *Advanced numerical modeling and data assimilation techniques for tropical cyclone prediction* (chap 1). Dordrecht, Netherlands: Springer. https://doi.org/10.5822/978-94-024-0896-6_1

Meissner, T., Ricciardulli, L., & Wentz, F. J. (2017). Capability of the SMAP mission to measure ocean surface winds in storms. *Bulletin of the American Meteorological Society*, *98*(8), 1660–1677. https://doi.org/10.1175/BAMS-D-16-0052.1

Mohanty, U. C., & Gopalakrishnan, S. G. (Eds.), (2016). *Advanced numerical modeling and data assimilation techniques for tropical cyclone prediction*. Dordrecht, Netherlands: Springer. https://doi.org/10.5822/978-94-024-0896-6

Montgomery, M. T., & Smith, R. K. (2017). Recent developments in the fluid dynamics of tropical cyclones. *Annual Review of Fluid Mechanics*, *49*(1), 541–574. https://doi.org/10.1146/annurev-fluid-010816-060022

Murakami, H. (2014). Tropical cyclones in reanalysis data sets. *Geophysical Research Letters*, *41*(6), 2133–2141. https://doi.org/10.1002/2014GL059519

Quilfen, Y., Chapron, B., Elfouhaily, T., Katsaros, K., & Tournadre, J. (1998). Observation of tropical cyclones by high-resolution scatterometry. *Journal of Geophysical Research*, *103*(C4), 7767–7786. https://doi.org/10.1029/97JC01911

Reul, N., Chapron, B., Zabolotskikh, E., Donlon, C., Quilfen, Y., Guimbard, S., & Piolle, J. F. (2016). A revised L-band radio-brightness sensitivity to extreme winds under tropical cyclones: The five year SMOS-storm database. *Remote Sensing of Environment*, *180*, 274–291. https://doi.org/10.1016/j.rse.2016.03.011

Reul, N., Tenerelli, J., Chapron, B., Vandemark, D., Quilfen, Y., & Kerr, Y. (2012). SMOS satellite L-band radiometer: A new capability for ocean surface remote sensing in hurricanes. *Journal of Geophysical Research*, *117*, C02006. https://doi.org/10.1029/2011JC007474

Ruf, C. S., Atlas, R., Chang, P. S., Clarizia, M. P., Garrison, J. L., Gleason, S., … Zavorotny, V. U. (2016). New ocean winds satellite mission to probe hurricanes and tropical convection. *Bulletin of the American Meteorological Society*, *97*(3), 385–395. https://doi.org/10.1175/BAMS-D-14-00218.1

Unwin, M., Jales, P., Tye, J., Gommenginger, C., Foti, G., & Rosello, J. (2016). Spaceborne GNSS-reflectometry on TechDemoSat-1: Early mission operations and exploitation. *IEEE Journal of Selected Topics in Applied Earth Observations and Remote Sensing*, *9*(10), 4525–4539. https://doi.org/10.1109/JSTARS.2016.2603846

Zavorotny, V. U., Gleason, S., Cardellach, E., & Camps, A. (2014). Tutorial on remote sensing using GNSS bistatic radar of opportunity. *IEEE Geoscience and Remote Sensing Magazine*, *2*(4), 8–45. https://doi.org/10.1109/MGRS.2014.2374220